

Coherence of polaronic transport in layered metals

Urban Lundin* and Ross H. McKenzie

Department of Physics, University of Queensland, Brisbane Qld 4072, Australia

(Dated: November 15, 2018)

Layered systems shows anisotropic transport properties. The interlayer conductivity show a general temperature dependence for a wide class of materials. This can be understood if conduction occurs in two different channels activated at different temperatures. We show that the characteristic temperature dependence can be explained using a polaron model for the transport. The results show an intuitive interpretation in terms of coherent and incoherent quasi-particles within the layers. Further, we extract results for the magnetoresistance, thermopower, spectral function and optical conductivity for the model and discuss application to experiments.

PACS numbers: 71.38.Ht, 71.38.-k, 72.90.

I. INTRODUCTION

Layered materials show a range of interesting behavior, ranging from high temperature superconductivity to giant and colossal magneto-resistance. A common feature of some of these materials (see for example Ref. 1,2,3) is that they show a peak in the interlayer resistivity as a function of temperature. In some cases there is also a peak in the intralayer resistivity. We can identify different temperature scales, from experiment. T_{\perp}^{\max} determines the maxima in the interlayer resistivity. T_{\parallel}^{\max} determines the maxima in the intralayer resistivity. Besides this, recent angle resolved photoemission (ARPES) experiments⁴ concluded that the peak in the interlayer resistivity is closely related to intralayer coherence, and that there is a crossover for the spectral function from being coherent to incoherent at a temperature T^{coh} . This idea that the scattering within the layers affect the transport between the layers have recently been investigated by Vozmediano et al.⁵. All of this can be ex-

TABLE I: Temperature scales in experiment for different materials. n.s. means that the peak is not seen in the experiment, indicating that, if it is there, it is higher than the temperature range scanned in the experiment, n.a. means the result is not available in our knowledge

Material	T_{\perp}^{\max} (K)	T_{\parallel}^{\max} (K)	T^{coh} (K)
$(\text{Bi}_{0.5}\text{Pb}_{0.5})_2\text{Ba}_3\text{Cu}_2\text{O}_y^a$	200	n.s.	~ 180
$\text{NaCo}_2\text{O}_4^a$	180	n.s.	~ 150
$\text{La}_{1.4}\text{Sr}_{1.6}\text{Mn}_2\text{O}_7^b$	100	270	n.a.
$\text{Sr}_2\text{RuO}_4^c$	130	n.s.	n.a.
$\text{TmBa}_2\text{Cu}_3\text{O}_{6.41}^d$	127	n.s.	n.a.
$(\text{TMTSF})_2\text{PF}_6^e$	90	n.s.	n.a.
$\kappa\text{-(BEDT-TTF)}_2\text{Cu}(\text{SCN})_2^f$	95	100	n.a.

^afrom Ref. 4

^bfrom Ref. 1

^cfrom Ref. 2

^dfrom Ref. 6

^efrom Ref. 7

^ffrom Ref. 8

plained if there are two mechanisms of transport.^{6,9} One, a coherent, dominates at low temperatures, while at ele-

vated temperatures an incoherent contribution starts to dominate. In this paper we will demonstrate that polaronic transport can be the mechanism providing this physics. This gives an intuitive explanation for the different temperature scales associated with transport and coherence. We extend the idea presented by Alexandrov and Bratkovsky¹⁰, and apply it to *layered* transport. In that paper they discussed (bi)polaron formation within giant magnetoresistance materials.

Another powerful tool when studying polaronic transport is to study the thermopower. At high temperatures the conductivity is activated and the resistivity shows an exponential temperature dependence with a gap E_{σ} , the thermopower usually shows a $1/T$ -behavior where the barrier is E_s . One signature of polaronic transport is that $E_s << E_{\sigma}$, whereas for normal semiconductors (where the transport is activated) we have $E_s = E_{\sigma}$ ¹¹. By comparing the high temperature electrical resistivity and thermopower a number of experimentalists have argued for the existence of small polarons in LaMnO_3 -compounds^{12,13,14}. Further evidence for small polarons can be found in neutron scattering data, where the polaron induces a local deformation of the lattice^{15,16,17}. Measurements of thermopower in different directions in an organic quasi-two-dimensional crystal found different behaviour between the interlayer thermopower and the interlayer one¹⁸. Further the presence of polarons was confirmed by photoemission experiments¹⁹.

The approach we present is based on known approximations for the polarons^{20,21}. Recent dynamical mean field (DMFT) calculations made on the transport of small polarons²² indicate that the approximations we are going to use overestimates the resistivity, and the exact functional behavior of the resistivity. The results of Fratini et al.²² shows that there are two temperature regions. One, semiconducting region where transport is heavily influenced by phonon fluctuations. Then a non-adiabatic regime, which compares mostly to the small polaron regime in the Holstein model. Here, however, we are more concerned with transitions between different regions of small polaron transport, not so much with the exact details, and it seems that the approximations we use does capture the essential physics. We do not claim

that polarons are responsible for all the observed effects, simply that it can provide some insight into the physics of layered systems. For instance, for the manganites it seems that the double exchange model is the preferred one (see Ref. 23 and references therein), although another explanation, in terms of a carrier density collapse due to bipolarons and their magnetic features²⁴ is gaining interest. Even the thermopower seems to be consistent with this model²⁵. There are also theories using a combination of double exchange models and polarons for the localized structure²⁶. A shorter presentation of some of the result from this paper has been previously published²⁷. We have also investigated the problem of angular magnetoresistance oscillations in layered metals arising from incoherence²⁸.

The layout of the paper is as follows, in section II we present the model and the small polarons are introduced in section III with the decay and Green function. In section IV we turn to the transport properties for the intralayer and interlayer currents and thermopower. Last we conclude with a calculation of the optical properties, section IV D, and a special case of the magnetoresistance in section IV E.

II. MODEL HAMILTONIAN

We start with a Holstein model²⁹ for an infinite system where the electrons interact with bosons. The Hamiltonian is

$$\mathcal{H} = \sum_i \epsilon^0 c_i^\dagger c_i + \sum_{\mathbf{q}} \hbar \omega_{\mathbf{q}} a_{\mathbf{q}}^\dagger a_{\mathbf{q}} + \sum_{\langle i\eta \rangle} t_{i\eta} c_\eta^\dagger c_i + \sum_{i,\mathbf{q}} M_{\mathbf{q}} c_i^\dagger c_i e^{i\mathbf{q} \cdot \mathbf{R}_i} (a_{\mathbf{q}} + a_{-\mathbf{q}}^\dagger), \quad (1)$$

where ϵ^0 is the on-site energy, $\omega_{\mathbf{q}}$ is the dispersion of the bosons, $t_{i\eta}$ is the hopping integral between neighboring sites i and η , $M_{\mathbf{q}}$ is the coupling between the bosons and the electrons. We want to emphasize that we will talk about bosons, since the theory will look the same for all types of bosons with a coupling given in the Hamiltonian above. The bosons can be phonons, spin-waves, plasmons, or any other type fulfilling bosonic commutation rules. Since we want to study layered systems we split the hopping into parallel and perpendicular to the layers, t_{\parallel} and t_{\perp} respectively, where $t_{\parallel} \gg t_{\perp}$. We only include hopping between nearest neighbors, both for the intra- and interlayer hopping. This enables us to write the Hamiltonian in a way more adapted for the layered case, shown in Fig. 1. The nature of the transport depends on how t_{\parallel} and t_{\perp} compares with Γ , the scattering rate due to the bosons. We assume that that $\Gamma > t_{\perp}$, so that the interlayer transport can be described by considering two decoupled layers. Meaning that the electrons scatters many times within the layers before jumping to the next^{2,5,27,28}. We assume that we can decouple the bosons within each layer separately, i.e., the bosons are localized

in each layer, the only interaction between bosons in different layers come from the electron tunneling, but this event occurs more seldom than the electron scattering of bosons in each layer. The Hamiltonian can be specified for this system. Two layers are coupled with a hopping Hamiltonian. Within each layer the electrons can hop but there is a coupling to a bosonic degree of freedom in each layer. We then use the Hamiltonian:

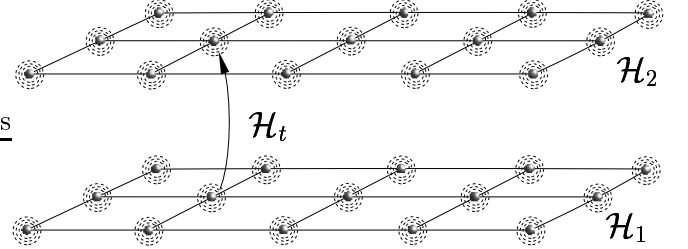


FIG. 1: We model the two coupled layers as anisotropic 3D system. Within each layer the electrons couple to bosons to potentially form small polarons. This is described by the Hamiltonians \mathcal{H}_1 and \mathcal{H}_2 . The two layers are coupled by a direct hopping term, \mathcal{H}_t .

$$\mathcal{H} = \mathcal{H}_1 + \mathcal{H}_2 + \mathcal{H}_t$$

where

$$\begin{aligned} \mathcal{H}_1 &= \sum_i \epsilon^0 c_i^\dagger c_i + \sum_{\mathbf{q}} \hbar \omega_{\mathbf{q}} a_{\mathbf{q}}^\dagger a_{\mathbf{q}} + t_{\parallel} \sum_{\langle i\eta \rangle} c_\eta^\dagger c_i + \sum_{i,\mathbf{q}} M_{\mathbf{q}} c_i^\dagger c_i e^{i\mathbf{q} \cdot \mathbf{R}_i} (a_{\mathbf{q}} + a_{-\mathbf{q}}^\dagger), \\ \mathcal{H}_2 &= \sum_j \epsilon^0 d_j^\dagger d_j + \sum_{\mathbf{p}} \hbar \omega_{\mathbf{p}} b_{\mathbf{p}}^\dagger b_{\mathbf{p}} + t_{\parallel} \sum_{\langle j\delta \rangle} d_\delta^\dagger d_j + \sum_{j,\mathbf{p}} M_{\mathbf{p}} d_j^\dagger d_j e^{i\mathbf{q} \cdot \mathbf{R}_j} (b_{\mathbf{p}} + b_{-\mathbf{p}}^\dagger), \\ \mathcal{H}_t &= t_{\perp} \sum_i (c_i^\dagger d_i + \text{h.c.}). \end{aligned}$$

Here, and below, $\mathbf{q}, c, i, a, 1$ refers to one layer, and $\mathbf{p}, d, j, b, 2$ to the other one.

III. SMALL POLARONS

First we focus on the properties of the two layers separately, i.e., we ignore the hopping term, \mathcal{H}_t between the layers. We perform a Lang-Firsov transformation³⁰ to diagonalize the Hamiltonian, excluding the hopping term, defined above, in each layer. Then $c_i \rightarrow \tilde{c}_i = c_i X_i$, and $d_j \rightarrow \tilde{d}_j = d_j Y_j$ where

$$\begin{aligned} X_i &= \exp \left[\sum_{\mathbf{q}} e^{i\mathbf{q} \cdot \mathbf{R}_i} \frac{M_{\mathbf{q}}}{\hbar \omega_{\mathbf{q}}} (a_{\mathbf{q}} - a_{-\mathbf{q}}^\dagger) \right], \\ Y_j &= \exp \left[\sum_{\mathbf{p}} e^{i\mathbf{p} \cdot \mathbf{R}_j} \frac{M_{\mathbf{p}}}{\hbar \omega_{\mathbf{p}}} (b_{\mathbf{p}} - b_{-\mathbf{p}}^\dagger) \right] \end{aligned} \quad (2)$$

are the polaron operators²⁰ for the first and second layer respectively. Further, $a_i \rightarrow a_i - \frac{M_{\mathbf{q}}}{\omega_0} c_i^\dagger c_i$. The Hamiltonian is transformed to $\bar{\mathcal{H}} = e^S \mathcal{H} e^{-S}$ where $S =$

$\frac{M}{\hbar\omega_0} \sum_i c_i^\dagger c_i (a_i^\dagger - a_i)$. The Hamiltonian becomes

$$\begin{aligned} \bar{\mathcal{H}} = & \sum_{\mathbf{q}} \hbar\omega_{\mathbf{q}} a_{\mathbf{q}}^\dagger a_{\mathbf{q}} + \sum_{\mathbf{p}} \hbar\omega_{\mathbf{p}} b_{\mathbf{p}}^\dagger b_{\mathbf{p}} - \sum_j \Delta d_j^\dagger d_j - \sum_i \Delta c_i^\dagger c_i \\ & + t_{\parallel} \sum_{i,\eta} (c_{i+\eta}^\dagger c_i X_{i+\eta}^\dagger X_i + \text{h.c.}) + t_{\parallel} \sum_{j,\delta} (d_{j+\delta}^\dagger d_j Y_{j+\delta}^\dagger Y_j + \text{h.c.}) \\ & + t_{\perp} \sum_{i,j} (c_i^\dagger d_j X_i^\dagger Y_j + \text{h.c.}), \end{aligned}$$

where

$$\Delta = \sum_{\mathbf{q}} \frac{M_{\mathbf{q}}^2}{\hbar\omega_{\mathbf{q}}} - \epsilon^0, \quad (4)$$

is the polaron binding energy. The intralayer hopping terms can be treated by adding and subtracting to the Hamiltonian a term³¹

$$\mathcal{H}_{sp} \equiv t_{\parallel} \sum_{\langle ij \rangle} \langle X_i X_j^\dagger \rangle c_i^\dagger c_j \equiv \sum_{\mathbf{k}} \epsilon_{\mathbf{k}} c_{\mathbf{k}}^\dagger c_{\mathbf{k}} \quad (5)$$

where $\langle \dots \rangle$ denotes a thermal average over boson states and this term describes a tight-binding band of small polarons for a square lattice within each layer^{30,31}

$$\epsilon_{\mathbf{k}} = \epsilon^0 - e^{-N^{-1} \sum_{\mathbf{q}} \left(\frac{M_{\mathbf{q}}}{\hbar\omega_{\mathbf{q}}} \right)^2 (1+2n_B)} t_{\parallel} [\cos(k_x a) + \cos(k_y a)], \quad (6)$$

where a is the lattice constant within the layers, N is the number of sites in one layer, and $n_B(T) = (\exp(\hbar\omega_{\mathbf{q}}/k_B T) - 1)^{-1}$ is the Bose function. We see that the quasi-particles are described by an tight binding energy, where the bandwidth is reduced due to the polaron formation. Polaron transport narrowing has been seen experimentally in muon-experiments.³²

There is then a residual interaction³¹ between the polarons and the bosons which is described by

$$\bar{\mathcal{H}}_{p-b} = t_{\parallel} \sum_{\langle ij \rangle} [X_i X_j^\dagger - \langle X_i X_j^\dagger \rangle] c_i^\dagger c_j, \quad (7)$$

and leads to scattering of the small polarons.

A. Decay of the quasi-particles

Later we will need the decay, Γ , so we start by calculating it. We will calculate the first contribution to the self energy in one layer by a method similar to the one used by Alexandrov and Mott³¹. The first non-zero contribution to the imaginary part of the self-energy, Σ , comes when the polaron emits one boson and absorb one boson. This process is shown in Fig. 2, and is induced by the polaron-boson scattering from Eq. (7). By using Fermi's Golden rule we get an expression for the decay:

$$\Gamma = 2\pi \sum_{\mathbf{q}, \mathbf{q}'} |\langle n_{\mathbf{q}} - 1, n_{\mathbf{q}'+1}; \mathbf{k} + \mathbf{q} - \mathbf{q}' | \mathcal{H}_{p-b} | n_{\mathbf{q}}, n_{\mathbf{q}'}; \mathbf{k} \rangle|^2 \times \delta(\epsilon_{\mathbf{k}} - \epsilon_{\mathbf{k}+\mathbf{q}-\mathbf{q}'}) \quad (8)$$

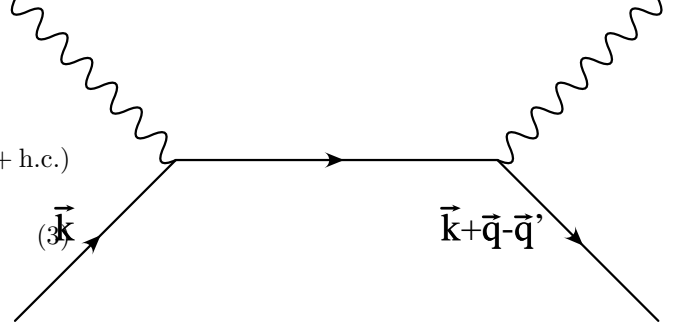


FIG. 2: Diagram describing the first contribution to the polaron decay, Γ . The polaron emits and absorbs one boson, changing its momenta.

Here, $\bar{\mathcal{H}}_{p-b}$ is the polaron-boson interaction in Eq. (7). Using this Hamiltonian we get that

$$\begin{aligned} \langle n_{\mathbf{q}} - 1, n_{\mathbf{q}'+1}; \mathbf{k} + \mathbf{q} - \mathbf{q}' | \bar{\mathcal{H}}_{p-ph} | n_{\mathbf{q}}, n_{\mathbf{q}'}; \mathbf{k} \rangle = & \frac{4t_{\parallel}}{N} \sqrt{n_{\mathbf{q}}} \sqrt{n_{\mathbf{q}'} + 1} \left(\frac{M_{\mathbf{q}}}{\hbar\omega_{\mathbf{q}}} \right) \left(\frac{M_{\mathbf{q}'}}{\hbar\omega_{\mathbf{q}'}} \right) \langle \mathbf{k} + \mathbf{q} - \mathbf{q}' | c_{\mathbf{k}+\mathbf{q}-\mathbf{q}'}^\dagger c_{\mathbf{k}} | \mathbf{k} \rangle \\ & \times \delta_{\mathbf{q}-\mathbf{q}'}. \end{aligned} \quad (9)$$

To simplify this to get a energy independent expression we use a energy independent density of states and assume a \mathbf{k} -independent coupling between the electrons and the bosons. We only consider a single frequency ω_0 for reasons of simplicity; it allows us to express some of our results in an analytical form. Then we can define the dimensionless coupling

$$g \equiv \left(\frac{M}{\hbar\omega_0} \right)^2$$

that will enter our equations later. We require that $g \gtrsim 1$ in order for small polaronic effects to be important.⁴³ Using this, we get that

$$\tau^{-1} = W g^2 n_B (1 + n_B), \quad (10)$$

where $W = 4\tilde{t}_{\parallel}$ is the polaron bandwidth, which is subject to narrowing due to the renormalization of the hopping $t \rightarrow \tilde{t}_{\parallel} \equiv t_{\parallel} e^{-g(1+2n_B)}$.

B. Green function in the layer

Let us start by calculating the *electron* Green function (GF) within one layer, ignoring the coupling between the layers ($t_{\perp} = 0$). This gives us valuable information on coherence of the quasi-particles, and can be compared to angle resolved photo-emission spectra (ARPES). After performing the Lang-Firsov transformation the small polaron GF is

$$\begin{aligned} G^0(\mathbf{k}, \tau) &= -i\Theta(\tau) \frac{1}{N} \sum_{i,i'} e^{i\mathbf{k} \cdot (\mathbf{R}_i - \mathbf{R}_{i'})} \langle T_{\tau} c_i(\tau) c_{i'}^\dagger(0) \rangle \\ &= -i\Theta(\tau) e^{(\epsilon_{\mathbf{k}} - i\Gamma)i\tau/\hbar}. \end{aligned}$$

To get the electron GF we have to convolute this GF with the average over two polaron operators $\langle TX_i^\dagger(t)X_{i'}(0)\rangle \equiv \Phi_{ii'}(t)$. This average can be decoupled and written as an exponential,^{20,30}

$$\Phi_{ii'}(t) = e^{-g(1/2+n_B)} \times \exp \left\{ g \sum_{\mathbf{q}} \cos[\mathbf{q} \cdot (\mathbf{R}_i - \mathbf{R}_{i'})][(1+n_B)e^{-i\omega t} + n_B e^{i\omega t}] \right\}$$

After Fourier transforming the average of the polaron operators, giving a sum of delta functions, we will have a convolution

$$G(\mathbf{k}, i\omega_n) = \frac{1}{N} \sum_{\omega_{n'}, \mathbf{R}_m, \mathbf{k}'} \Phi(\mathbf{R}_m, \omega_{n'} - \omega_n) G^0(\mathbf{k}', \omega_{n'}) e^{i(\mathbf{k}-\mathbf{k}' \cdot \mathbf{R}_m)}$$

After some algebra we come to the following expression

$$G(\mathbf{k}, i\omega_n) = e^{-g(1+2n_B)} \frac{1}{N} \sum_{\mathbf{R}_m, \mathbf{k}'} e^{i(\mathbf{k}-\mathbf{k}') \cdot \mathbf{R}_m} \times \sum_{l=-\infty}^{\infty} \frac{I_l [2g \sum_{\mathbf{q}} \cos(\mathbf{q} \cdot \mathbf{R}_m) \sqrt{n_B(1+n_B)}]}{i\omega_n - \epsilon_{\mathbf{k}'} + l\hbar\omega_0 + i\Gamma}$$

Here I_l indicates a modified Bessel function of order l . Performing the summation over \mathbf{R}_m , care has to be taken when considering the $l = 0$ term, we get the final result for the GF

$$G(\mathbf{k}, \omega) = e^{-g(1+2n_B)} \left\{ \frac{1}{\omega - \epsilon_{\mathbf{k}} + i\Gamma} + \sum_{\mathbf{k}'} \frac{I_0 [2g \sqrt{n_B(1+n_B)}] - 1}{\omega - \epsilon_{\mathbf{k}'} + i\Gamma} + \sum_{\mathbf{k}', l \neq 0} \frac{I_l [2g \sqrt{n_B(1+n_B)}] e^{-l\hbar\omega_0\beta/2}}{\omega - \epsilon_{\mathbf{k}'} + l\hbar\omega_0 + i\Gamma} \right\}. \quad (13)$$

Note that we have written the GF as a sum of a coherent and an incoherent part. This can be compared to the zero temperature result by Alexandrov and Mott³¹. At $T = 0$ there are no bosons to absorb and only $l \geq 0$ contributes to the GF. Also, we can compare this to the nonzero temperature GF by Ciuchi *et al.*³³. The first line is dependent on \mathbf{k} , thereby describing a coherent part. There will be a well-defined quasiparticle peak at $\omega = \epsilon_{\mathbf{k}}$, with a spectral weight of $e^{-g(1+2n_B)}$. The second and third lines contains a sum over intralayer momentum and are therefore independent of \mathbf{k} , they are incoherent. The two contributions have different temperature dependence, the coherent dominates at low temperature, and the incoherent at high temperature. This means that there is a crossover from coherent intralayer motion at low temperature to incoherent intralayer motion at high temperatures. In Fig. 3 we show the spectral function

resulting from this GF at the Fermi wave-vector as a function of energy. The sum over \mathbf{k} is done by integrating over a flat density of states. This is what is measured in ARPES experiments like the one in reference 4 for $(\text{Bi}_{0.5}\text{Pb}_{0.5})_2\text{Ba}_3\text{Co}_2\text{O}_y$ and NaCo_2O_4 . Recently, similar features was seen in Sr_2RuO_4 .³⁴ The coherent contribution display a peak at the Fermi energy and \mathbf{k} -vector at low temperature, indicating a coherent quasi-particle. The peak disappears as the temperature is increased.

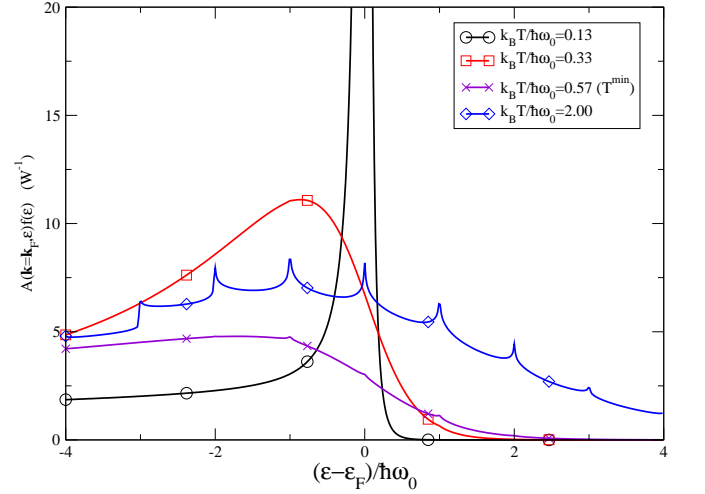


FIG. 3: The quasi-particle spectral function, $n_f(\epsilon) \text{Im}[G(\mathbf{k}_F, \epsilon)]$ for a electron-phonon coupling, $g = 1$, for different temperatures. The sum over \mathbf{k} is done by integrating over the density of states, which we assume is flat with a bandwidth $W = 77\hbar\omega_0$. There are two contributions to the spectra function, one coherent dominating at low temperatures, and one incoherent dominating at high temperatures. Similar behavior have been seen experimentally⁴.

crossover temperature when the contribution from the incoherent starts to dominate over the incoherent one. This will take place when

$$k_B T^* \sim \frac{\hbar\omega_0}{2g}. \quad (14)$$

Later we will see that this relates to the temperature dependence of the interlayer conductivity in a special way.

IV. TRANSPORT PROPERTIES

Let us now turn to the transport properties of the layered material which is described by the layered Hamiltonian defined above. At an applied voltage V , the current is given by the current-current correlation function from the Kubo formula²⁰

$$I_{\mu\nu}(eV) = \frac{2e}{h} \text{Im} \left\{ \int_0^\beta dt e^{ieVt} \langle T \hat{j}_\mu(t) \hat{j}_\nu^\dagger(0) \rangle \right\}, \quad (15)$$

where \hat{j} is the current operator. μ and ν are directions in the crystal. For our system, including polarons, the current operator for nearest neighbor hopping is

$$(j_a, j_b, j_c) = -\frac{ie}{\hbar} \left[t_{\parallel} \sum_{i,\eta} (\vec{R}_{i+\eta}^{\parallel} - \vec{R}_i^{\parallel}) c_{i+\eta}^{\dagger} c_i X_{i+\eta}^{\dagger} X_i + t_{\parallel} \sum_{j,\eta} (\vec{R}_{j+\eta}^{\parallel} - \vec{R}_j^{\parallel}) d_{j+\eta}^{\dagger} d_j Y_{j+\eta}^{\dagger} Y_j + t_{\perp} \sum_{j,\delta} (\vec{R}_{j+\delta}^{\perp} - \vec{R}_j^{\perp}) d_{j+\delta}^{\dagger} c_j Y_{j+\delta}^{\dagger} X_j \right], \quad (16)$$

The first term corresponds to hopping in layer 1, the second term to hopping in layer 2, and the third to hopping between adjacent positions in the two layers. Since we also are going to study thermopower we give the expression for the energy current in the same model

$$(j_a^e, j_b^e, j_c^e) = -\frac{ie}{\hbar} \left[\frac{t_{\parallel}\epsilon}{2} \sum_{i,\eta} (\vec{R}_{i+\eta}^{\parallel} - \vec{R}_i^{\parallel}) c_{i+\eta}^{\dagger} c_i X_{i+\eta}^{\dagger} X_i + \frac{t_{\parallel}\epsilon}{2} \sum_{j,\eta} (\vec{R}_{j+\eta}^{\parallel} - \vec{R}_j^{\parallel}) d_{j+\eta}^{\dagger} d_j Y_{j+\eta}^{\dagger} Y_j + \frac{t_{\perp}\epsilon}{2} \sum_{j,\delta} (\vec{R}_{j+\delta}^{\perp} - \vec{R}_j^{\perp}) d_{j+\delta}^{\dagger} c_j Y_{j+\delta}^{\dagger} X_j \right], \quad (17)$$

and ϵ is the energy of the quasi-particle. Let us separate the current within the layers and perpendicular to the layers, since they usually show a different behaviour in experiment.

A. Current within the layers

In this section we will calculate the current within the layers. We split the calculation into two regimes because if we use Eq. (16) directly in Eq. (15), the result is too complicated to decouple, so we split the calculation into low and high temperatures, where different parts of the Hamiltonian dominates, and we can use perturbation theory.

1. Low Temperatures

At low temperatures the transport within the layers is coherent. If the layers are metallic we can treat them in a Fermi-liquid manner and use that the conductivity depends on the scattering rate via the scattering time, $\tau = h/\Gamma$,

$$\sigma_{\parallel} = \frac{e^2}{2\pi^2} \int v(\mathbf{k}) \bar{v}(\mathbf{k}) \left(-\frac{\partial f}{\partial \epsilon} \right) \tau(\mathbf{k}) d^2k. \quad (18)$$

The decay is calculated as usual from the imaginary part of the self energy, and is given in Eq. (10). We use the tight binding approximation, Eq. (6), to get the quasi-particle velocity, $\mathbf{v}(\mathbf{k}) = \frac{\nabla_{\mathbf{k}}\epsilon}{\hbar}$, in one direction and get the conductivity,

$$\sigma_{\parallel}^{xx} = \frac{e^2}{\pi h} \frac{\beta \tilde{t}_{\parallel} a^2}{g^2 n_B (1 + n_B)} \times \int_{-2\pi}^{2\pi} dx dy \frac{\sin^2(x)}{1 + \cosh[\beta(\epsilon_0 + \tilde{t}_{\parallel} \cos(x) + \tilde{t}_{\parallel} \cos(y) - \mu)]}. \quad (19)$$

2. High Temperatures

At high temperatures the polarons are localized, the bandwidth disappears, and the hopping, t_{\parallel} , is the perturbation. Utilizing Eq. (15) for the current, we decouple the electron operators to polaron GFs in each layer, $G = (\omega - \Delta + \Sigma + i\Gamma)^{-1}$. Note that there is no \mathbf{k} -dependence for the polaron GFs since they are localized at an energy $\Delta = \epsilon_0 - g\hbar\omega_0 < 0$. The calculation of the GF in perturbation theory is described in Appendix A. The 4 X -operators are decoupled as in Ref. 20 into diagonal (no change of boson state) and non-diagonal transitions (when the boson-state changes in the hop). The result for the non-diagonal transitions is

$$\langle T_{\tau} X^{\dagger}(\tau) X(\tau) X^{\dagger}(0) X(0) \rangle_{\omega} = e^{-2g(1+2n_B)} \sum_{l=-\infty}^{\infty} \left\{ \int_{-\infty}^{\infty} I_l \left[4g\sqrt{n_B(1+n_B)} \right] e^{-l\hbar\omega_0\beta/2} e^{il\omega_0 t} - 1 \right\} \quad (20)$$

For the diagonal part the four X -operators decouple and cancels the -1 term above when added together. Combining the two correlators and taking the imaginary part we convolute the two Fourier transforms similarly to what was done for the GF above, so that we get for the current:

$$I_{\parallel}(\omega) = \frac{2e}{h} t_{\parallel}^2 d^2 e^{-2g(1+2n_B)} \int_{-\infty}^{\infty} \frac{d\epsilon}{2\pi} A(\epsilon) \times \sum_{l=-\infty}^{\infty} I_l \left[4g\sqrt{n_B(1+n_B)} \right] e^{-l\hbar\omega_0\beta/2} A(\epsilon + \omega + l\hbar\omega_0) \times [n_F(\epsilon) - n_F(\epsilon + \omega + l\hbar\omega_0)]. \quad (21)$$

The conductance is obtained as usual as $\sigma_{\parallel} = e \left. \frac{dI_{\parallel}}{d(\omega)} \right|_{\omega=0}$.

The conductivity can now be plotted. The metallic, low temperature, part decreases with increasing temperature and the insulating, high temperature, phase takes over as temperature is increased. There is a peak in the resistivity and a crossover from coherent to incoherent transport, described by Eq. (19) and Eq. (21) respectively. We did similar plots for a range of coupling constants, g , and saw that the intralayer crossover occurs at

a temperature given by

$$k_B T_{\parallel}^{\max} \sim 2 \frac{\hbar \omega_0}{g}. \quad (22)$$

We have used the same decay, Γ , for both the low and high-temperature limits. This approximation assumes that the dominant part of the scattering of the carriers in both limits is the electron-boson coupling. The results are shown below in the figures below.

B. Current perpendicular to the layers

Let us now turn to the current perpendicular to the layers. The current operator for an applied field in the perpendicular direction in a nearest neighbor hopping model (from layer 1 to 2) is given in Eq. (16). We assume that the hopping between the layers only take place between nearest neighbors, see Fig. 1. Then, $(\mathbf{R}_{j+\delta} - \mathbf{R}_j)$ is the distance between the two layers, d , since $\delta = 1$ for nearest neighbor hopping. The Kubo formula, Eq. (15), gives that we have, to second order in t_{\perp} ,

$$I_{\perp}(eV) = \frac{2e}{\hbar} t_{\perp}^2 d^2 \sum_{j,j_1} \int_0^{\beta} d\tau e^{ieV\tau} \left\langle T_{\tau} c_j^{\dagger}(\tau) d_{j_1}(\tau) d_j^{\dagger}(0) c_{j_1}(0) \right\rangle \times \left\langle T_{\tau} Y_{j_1}^{\dagger}(\tau) Y_j(\tau) X_j^{\dagger}(0) X_{j_1}(0) \right\rangle.$$

We decouple the operators in the first and second layer respectively. This means that the Fourier transformed averages of the electron operators gives rise to polaron Green functions

$$\left\langle T c_j^{\dagger}(t) c_{j_1}(0) \right\rangle \rightarrow G_1^0(\mathbf{k}, ip_n),$$

$$\left\langle T d_{j_1}(t) d_j^{\dagger}(0) \right\rangle \rightarrow G_2^0(\mathbf{p}, ip_n - i\omega).$$

The average of the polaron-operators (X, Y) can be decoupled for the two layers separately, and written as an exponential $\Phi(t)$,^{20,30} as done for the GF above. Since the coupling in all layers are the same, $M_1 = M_2$, we can either combine the two averages of the polaron operators into one exponential ($\Phi(t) * \Phi(t) = (\Phi(t))^2$) or keep them as two separate. Then we can perform the Fourier transform $\tau \rightarrow \omega$, and if we assume that the GFs has an imaginary part, as above, we get the following for the (2B) interlayer tunneling current

$$I_{\perp}(eV) = \frac{2e}{\hbar} t_{\perp}^2 d^2 e^{-2g(1+2n_B)} \left\{ \int_{-\infty}^{\infty} \frac{d\epsilon}{2\pi} \sum_{\mathbf{k}} A_1^0(\mathbf{k}, \epsilon) A_2^0(\mathbf{k}, \epsilon + eV) [f(\epsilon) - f(\epsilon + eV)] + \left(I_0 \left[4g\sqrt{n_B(1+n_B)} \right] - 1 \right) \int_{-\infty}^{\infty} \frac{d\epsilon}{2\pi} \sum_{\mathbf{k}} A_1^0(\mathbf{k}, \epsilon) \sum_{\mathbf{p}} A_2^0(\mathbf{p}, \epsilon + eV) [f(\epsilon) - f(\epsilon + eV)] + \sum_{l=-\infty}^{\infty} I_l \left[4g\sqrt{n_B(1+n_B)} \right] e^{-l\hbar\omega_0\beta/2} \int_{-\infty}^{\infty} \frac{d\epsilon}{2\pi} \sum_{\mathbf{k}} A_1^0(\mathbf{k}, \epsilon) \sum_{\mathbf{p}} A_2^0(\mathbf{p}, \epsilon + eV + l\hbar\omega_0) [f(\epsilon) - f(\epsilon + eV + l\hbar\omega_0)] \right\} \quad (24)$$

\mathbf{k} belongs to the first layer, and \mathbf{p} to the second. A_1^0 and A_2^0 are the spectral functions for the electron GFs in each layer respectively,

$$A_1^0(\mathbf{k}, \epsilon) = \frac{\Gamma}{(\epsilon - \epsilon_{\mathbf{k}})^2 + \Gamma^2}, \quad (25)$$

$$A_2^0(\mathbf{p}, \epsilon) = \frac{\Gamma}{(\epsilon - \epsilon_{\mathbf{p}})^2 + \Gamma^2}. \quad (26)$$

The index l is a combined index for the number of bosons emitted or absorbed in layer 1 and 2 combined

To illustrate this, consider what would be obtained if we had not combined the two exponentials, the result would be:

$$\begin{aligned}
I_{\perp}(eV) \propto & 2t_{\perp}^2 e^{-\sum_{\mathbf{q}} \left(\frac{M_{\mathbf{q}}}{\hbar\omega_{\mathbf{q}}} \right)^2 (1+2n_B) - \sum_{\mathbf{p}} \left(\frac{M_{\mathbf{p}}}{\hbar\omega_{\mathbf{p}}} \right)^2 (1+2n_B)} \prod_{\mathbf{q}, \mathbf{p}} \sum_{l, l'=-\infty}^{\infty} \\
& \times \int_{-\infty}^{\infty} \frac{d\epsilon}{2\pi} A_2(\epsilon - l'\hbar\omega_{\mathbf{q}}) A_1(\epsilon + eV + l\hbar\omega_{\mathbf{p}}) [n_F(\epsilon - l'\hbar\omega_{\mathbf{q}}) - n_F(\epsilon + eV + l\hbar\omega_{\mathbf{p}})] \\
& \times I_l \left(2 \left(\frac{M_{\mathbf{p}}}{\hbar\omega_{\mathbf{p}}} \right)^2 \sqrt{n_B(1+n_B)} \right) I_{l'} \left(2 \left(\frac{M_{\mathbf{q}}}{\hbar\omega_{\mathbf{q}}} \right)^2 \sqrt{n_B(1+n_B)} \right) e^{-\beta/2(l\hbar\omega_{\mathbf{p}} + l'\hbar\omega_{\mathbf{q}})}. \quad (27)
\end{aligned}$$

l belongs to the first layer and counts the number of bosons attached to the electron, l' refers in a similar fashion to the second layer. The connection between Eq. (24), and Eq. (27) can be found from the identity for the Bessel functions

$$\sum_{l, l'=-\infty}^{\infty} I_{l-l'}(x_1) I_{l'}(x_2) = \sum_{l=-\infty}^{\infty} I_l(x_1 + x_2). \quad (28)$$

The expression for the current, Eq. (24), has a contribution from coherent and two from incoherent transport. Note the similarity in structure of Eq. (24) to the expression for the GF, Eq. (13). The first term corresponds to transport which conserves the intralayer momentum in the tunneling process. This is seen since the crystal momentum \mathbf{k} is the same for the spectral function for the two different layers. For the other terms, the intralayer momentum is not conserved, (in each layer the sums over the momentum are separate). The second row corresponds to transport when the net number of bosons in the system is unchanged. When the quasiparticle tunnels it leaves behind the cloud of bosons in one layer and attaches to a replica of bosons in the second layer. The third row describes transport when a net number of bosons is absorbed ($l > 0$) or emitted ($l < 0$), thus changing the energy of the polaron in the hop between the two layers. In a recent paper²⁸ we established a connection between the intralayer coherence and the appearance of dips in the angular magnetoresistance, the so called "magic angles". We showed that a contribution from incoherent jumps between highly conducting one-dimensional strands of molecules gives a natural explanation of the phenomena observed in the magnetoresistance. At low temperature the coherent part dominates but at high temperature (high compared to the boson energy, $\hbar\omega_0$, $k_B T > \hbar\omega_0$) the incoherent mechanism of transport will dominate. Thus, there is a *crossover* from coherent to incoherent transport. The crossover temperature is fixed by having equal contribution from the coherent and the incoherent contributions. Ignoring the contribution from the $l \neq 0$ terms in Eq. (24) we can get an approximate expression for the crossover temperature as:

$$k_B T^{\min} \sim \frac{\hbar\omega_0}{\sqrt[4]{2^3 g}} \sim 1.68 \frac{\hbar\omega_0}{g}. \quad (29)$$

From Eq. (24) we can extract the conductivity by a simple derivative $\sigma_{\parallel} = e \frac{dI_{\parallel}}{d(eV)} \Big|_{eV=0}$. In Fig. 4 we plot the conductivity as a function of temperature for one value of g . The crossover is clearly seen.

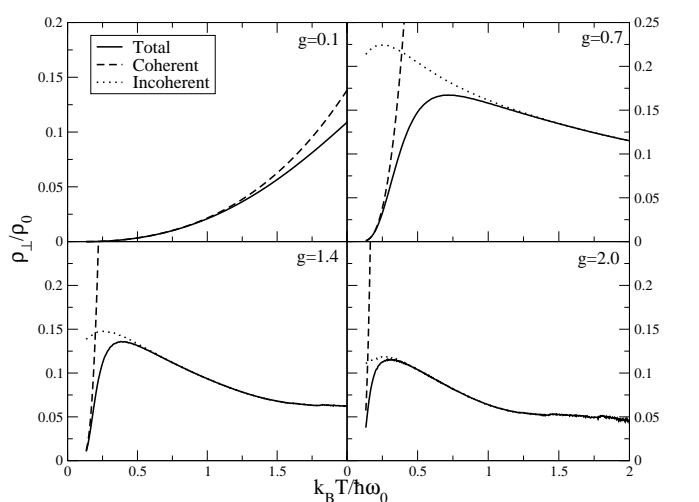


FIG. 4: Interlayer resistivity as a function of temperature for different values of the coupling g . At low temperatures, the transport is predominantly coherent, as seen from Eq. (24). Then, as the temperature is increased, the incoherent mechanism of transport take over. We have $\sigma_{\perp} = \sigma_{\perp}^{coh.} + \sigma_{\perp}^{inc.}$, the two contributions are shown separately and together in the plot. The crossover from coherent to incoherent transport is clearly seen. $\rho_0^{-1} = \frac{2e^2}{h} t_{\perp}^2 d^2$, $W = 77\hbar\omega_0$.

In general, the interlayer conductivity for identical decoupled layers is³⁵,

$$\sigma_{\perp} = \frac{2e^2}{h} t_{\perp}^2 \int d\epsilon \sum_{\mathbf{k}} |A(\mathbf{k}, \epsilon)|^2 \left[-\frac{df}{d\epsilon} \right], \quad (30)$$

where $A(\mathbf{k}, \epsilon)$ is the *electron* spectral function for a single layer. Directly substituting Eq. (13) in Eq. (30) we obtain the same result found from Eq. (24).

We can check the result by taking some limits in Eq. (24) When the temperature is zero, we get

$$\begin{aligned}\sigma_{\perp}(T=0) &= \frac{2e^2}{h} t_{\perp}^2 d^2 e^{-2g} \sum_{\mathbf{k}} \frac{A_1(\mathbf{k}, 0) A_2(\mathbf{k}, 0)}{2\pi} \\ &= \frac{2e^2}{2\pi h} t_{\perp}^2 e^{-2g} \frac{D(\epsilon=0)}{2\Gamma}.\end{aligned}\quad (31)$$

Thus, at low temperature when only the first (coherent) term contributes to the conductivity the temperature dependence of σ_{\perp} is governed by the temperature dependence of the decay, Γ , given by Eq. (10), for the polaron case. If we expand Eq. (24) for high temperatures the conductivity behaves approximately as:

$$\sigma_{\perp} \propto T^{-3/2}, \quad (32)$$

which is consistent with the equipartition theorem³⁶.

If we take the limit $g=0$ we get:

$$\begin{aligned}\sigma_{\perp}(g=0) &= \frac{2e^2}{h} t_{\perp}^2 d^2 \sum_{\mathbf{k}} \int_{-\infty}^{\infty} \frac{d\epsilon}{2\pi} A_1(\mathbf{k}, \epsilon) A_2(\mathbf{k}, \epsilon) \\ &\quad \times \beta n_F(\epsilon) [1 - n_F(\epsilon)],\end{aligned}\quad (33)$$

as expected from transport theory²⁰.

C. Thermopower

Let us now turn to calculating the thermopower for intralayer and interlayer transport. The thermopower is defined as a correlator, using the heat current instead of the electrical current in Eq. (15), (See Ref. 20)

$$L^{12} = \frac{2e}{h} \text{Im} \left\{ \int_0^{\beta} dt e^{i\omega t} \langle T \hat{j}_{\mu}^e(t) \hat{j}_{\nu}^e(0) \rangle \right\}, \quad (34)$$

and, using that the current-current correlator gives us L^{11} , and $\sigma = L^{11}/T$, we get

$$S = \frac{1}{T} \frac{L^{12}}{L^{11}} = \frac{1}{T^2} \frac{L^{12}}{\sigma}. \quad (35)$$

For the intralayer thermopower we consider the low and high temperature limits separately.

1. Low temperature intralayer thermopower

At low temperatures the correlator is similar to the one calculated for the intralayer low-temperature conductivity, except for an additional $\epsilon_k/2$ in the (energy)current operator. This factor only contributes an additional $\tilde{t}_{\parallel} \cos(k_x a)/2$ if we assume that we do the measurement along x . The result is that, for low temperatures, the thermopower is

$$S_{\parallel}^{\text{low}} = \frac{1}{T} \frac{\tilde{t}_{\parallel}}{2e} \frac{\int d^2 k f(\epsilon_{kk}) [1 - f(\epsilon_{kk})] \sin^2(k_x a) \cos(k_x a)}{\int d^2 k f(\epsilon_{kk}) [1 - f(\epsilon_{kk})] \sin^2(k_x a)}. \quad (36)$$

2. High temperature intralayer thermopower

At high temperatures, we can follow the same steps as for the intralayer current with the only difference that the energy operator is the current operator multiplied by $\frac{t_{\parallel}}{2}$. Then, in Eq. (35) the correlators cancel, and we simply end up with³⁷:

$$S_{\parallel}^{\text{high}} = \frac{t_{\parallel}}{2eT}. \quad (37)$$

The two results in the low and high temperature regions, Eq. (36) and Eq. (37) respectively, both falls off as $\frac{1}{T}$. This means that there would be no peak in the intralayer thermopower corresponding to any transition between coherent and incoherent transport. Therefore, the transition in the intralayer transport is more clearly seen in the electrical transport, not the thermopower. The $1/T$ -dependence is typical for polarons at high temperatures as seen, e.g., in $\text{La}_{2/3}\text{Ca}_{1/3}\text{MnO}_3$ films,³⁸ and $(\text{La},\text{Ca})\text{MnO}_3$.¹²

3. Interlayer thermopower

We follow the same steps as for the interlayer conductivity with the replacement of one current operator by one energy-current operator as in Eq. (34). The result for L^{12} is

$$\begin{aligned}
L_{\perp}^{12} = & \frac{2e}{h} t_{\perp}^2 e^{-2g(1+2n_B)} d^2 \left\{ \int_{-\infty}^{\infty} \frac{d\epsilon}{2\pi} \sum_{\mathbf{k}} \xi_{\mathbf{k}} A_1^0(\mathbf{k}, \epsilon) A_2^0(\mathbf{k}, \epsilon + eV) [f(\epsilon) - f(\epsilon + eV)] \right. \\
& + \left(I_0 \left[4g\sqrt{n_B(1+n_B)} \right] - 1 \right) \int_{-\infty}^{\infty} \frac{d\epsilon}{2\pi} \sum_{\mathbf{k}} \xi_{\mathbf{k}} A_1^0(\mathbf{k}, \epsilon) \sum_{\mathbf{p}} A_2^0(\mathbf{p}, \epsilon + eV) [f(\epsilon) - f(\epsilon + eV)] \\
& \left. + \sum_{l \neq 0}^{\infty} I_l \left[4g\sqrt{n_B(1+n_B)} \right] e^{-l\hbar\omega_0\beta/2} \int_{-\infty}^{\infty} \frac{d\epsilon}{2\pi} \sum_{\mathbf{k}} \xi_{\mathbf{k}} A_1^0(\mathbf{k}, \epsilon) \sum_{\mathbf{p}} A_2^0(\mathbf{p}, \epsilon + eV + l\hbar\omega_0) [f(\epsilon) - f(\epsilon + eV + l\hbar\omega_0)] \right\}. \tag{38}
\end{aligned}$$

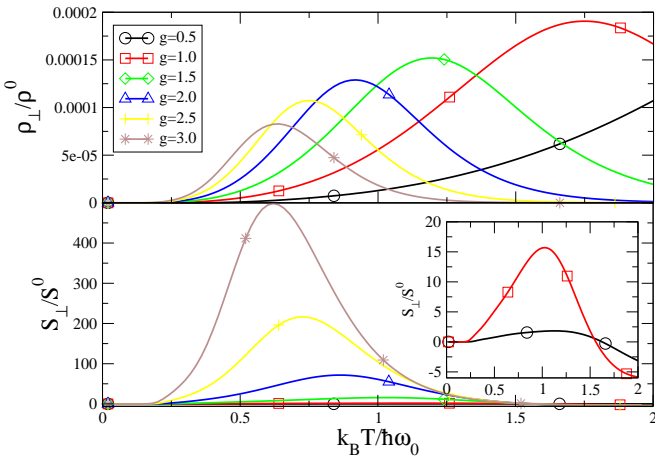


FIG. 5: The top panel shows the interlayer resistivity as a function of temperature for different electron-phonon coupling strengths, $\rho_0^{-1} = \frac{2e^2}{h} t_{\perp}^2 d^2$, $W = 160\hbar\omega_0$. The peak correspond to the transition between coherent and incoherent transport. The lower panel shows the interlayer thermopower, $S^0 = \frac{t_{\perp}}{2e}$. The peak in the thermopower occurs at a lower temperature than for the resistivity. The inset shows the thermopower for small electron-phonon coupling, note that it can change sign although we do not consider carriers of hole type here. At high temperatures, and strong electron-phonon coupling, the thermopower decays exponentially.

Here $\xi_{\mathbf{k}} = \epsilon_{\mathbf{k}} - \mu$. The thermopower is then given by Eq. (35). In Fig. 5 we make a comparative plot of the resistivity and the thermopower between the layers. For a Fermi-liquid the thermopower would fall off as $\frac{1}{T}$ at high temperatures (see, e.g., Salamon *et al.*¹¹), fitting a curve to our numerical results shows that our expression for the interlayer thermopower falls off *exponentially* instead.

D. Optical conductivity

The optical conductivity is given by calculating the derivative of the frequency dependent current $I_{\perp}(\omega)$ in Eq. (24) with respect to $\omega = eV$. Assuming that the following relations hold (when $\Gamma \ll W$)

$$\begin{aligned}
\int dx D(x) A(x, \epsilon) &= \int dx D(x) \frac{\Gamma}{(\epsilon - x)^2 + \Gamma^2} = D(\epsilon) \\
\int dx D(x) A(x, \epsilon) A(x, \epsilon + \omega) &= \\
\int dx D(x) \frac{\Gamma}{(\epsilon - x)^2 + \Gamma^2} \frac{\Gamma}{(\epsilon + \omega - x)^2 + \Gamma^2} &= \\
D(\epsilon) \frac{\Gamma}{\omega^2 + \Gamma^2}
\end{aligned}$$

We get that the full expression for the optical conductivity is:

$$\begin{aligned}
\sigma(\omega) = & \frac{2e^2}{h} t_\perp^2 d^2 e^{-2g(1+2n_B)} \left\{ \int_{-\infty}^{\infty} \frac{d\epsilon}{2\pi} D(\epsilon) \frac{\Gamma}{\omega^2 + \Gamma^2} \beta n_F(\epsilon + \omega) [1 - n_F(\epsilon + \omega)] \right. \\
& + \left(I_0 \left[4g\sqrt{n_B(1+n_B)} \right] - 1 \right) \int_{-\infty}^{\infty} \frac{d\epsilon}{2\pi} D(\epsilon) D(\epsilon + \omega) \beta n_F(\epsilon + \omega) [1 - n_F(\epsilon + \omega)] \\
& + \sum_{l=-\infty}^{\infty} I_l \left[4g\sqrt{n_B(1+n_B)} \right] e^{-l\hbar\omega_0\beta/2} \int_{-\infty}^{\infty} \frac{d\epsilon}{2\pi} D(\epsilon) D(\epsilon + \omega + l\hbar\omega_0) \beta n_F(\epsilon + \omega + l\hbar\omega_0) [1 - n_F(\epsilon + \omega + l\hbar\omega_0)] \\
& + \int_{-\infty}^{\infty} \frac{d\epsilon}{2\pi} D(\epsilon) \frac{2\Gamma\omega}{(\omega^2 + \Gamma^2)^2} [n_F(\epsilon) - n_F(\epsilon + \omega)] \\
& + \left(I_0 \left[4g\sqrt{n_B(1+n_B)} \right] - 1 \right) \int_{-\infty}^{\infty} \frac{d\epsilon}{2\pi} D(\epsilon) D'(\epsilon + \omega) [n_F(\epsilon) - n_F(\epsilon + \omega)] \\
& \left. + \sum_{l=-\infty}^{\infty} I_l \left[4g\sqrt{n_B(1+n_B)} \right] e^{-l\hbar\omega_0\beta/2} \int_{-\infty}^{\infty} \frac{d\epsilon}{2\pi} D(\epsilon) D'(\epsilon + \omega + l\hbar\omega_0) [n_F(\epsilon) - n_F(\epsilon + \omega + l\hbar\omega_0)] \right\}.
\end{aligned}$$

Here D' is the derivative of the density of states (which is zero for a constant DOS). In the figure for the optical conductivity, Fig. 6, we see that there is a large coherent Drude peak at low frequency, which disappears as the temperature increases, consistent with ex-

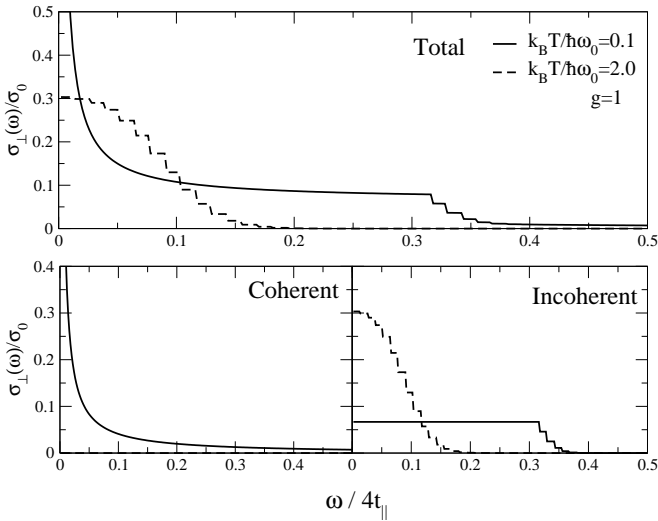


FIG. 6: The top panel shows the frequency dependence of the interlayer optical conductivity for two different temperatures. The Drude peak (at $\omega = 0$) disappears when coherence is lost, due to the destruction of coherent quasi-particles with increasing temperature. The two lower panels shows the optical conductivity divided into the two contributions, coherent and incoherent plotted for two different temperatures. The input density of state is flat with a bandwidth of $W = 77\hbar\omega_0$.

ance of the Drude peak is consistent with the peak in the spectral function disappearing, Fig. 3. Such a behavior has been observed³⁹ in Sr_2RuO_4 , where the Drude peak disappeared above 100K. Another system is $\text{La}_{0.825}\text{Sr}_{0.175}\text{MnO}_4$ where the Drude peak disappears

above 200K.⁴⁰

E. Interlayer Magnetoresistance for a field parallel to the layers

We can also make a statement about the magnetoresistance in a certain limit. If we apply a magnetic field, B , parallel to the layers (the x-y plane) there is an orbital effect on the paths of the electrons. This can be described by a shift in wave vector, $\mathbf{k} \rightarrow \mathbf{k} - \frac{e}{\hbar}\mathbf{A}$, where \mathbf{A} is the vector potential for the magnetic field. For a magnetic field in the x direction, when an electron tunnels between adjacent layers it undergoes a shift in the y -component of its wave vector by $-dB$ ³⁵. In the general expression Eq. (30) $|A(\mathbf{k}, \epsilon)|^2$ is replaced with an equation containing $A_1(\mathbf{k}, \epsilon)A_2(\mathbf{k} + \frac{e}{\hbar}dB\vec{y})$, since there will be a difference in the vector potential between the two layers.

However, since the incoherent part of the conductivity contains a summation over \mathbf{k} -space and is *independent* of \mathbf{k} , this will be unaffected by the magnetic field, i.e. $\sum_{\mathbf{p}} A_2^0(\mathbf{p} + \frac{e}{\hbar}dB\vec{y}, \epsilon + eV) = \sum_{\mathbf{p}} A_2^0(\mathbf{p}, \epsilon + eV)$ since the sum span over the first Brillouin zone.

Thus, we will have two contributions to the interlayer conductivity and one is B -independent:

$$\sigma_{\perp}(B) = \sigma_{\perp}^{\text{coh}}(B) + \sigma_{\perp}^{\text{incoh}}(B = 0). \quad (39)$$

$\sigma^{\text{coh}}(B)$ decreases with increasing magnetic field^{35,41}

$$\sigma_{\perp}^{\text{coh}}(B) = \frac{\sigma_{\perp}^{\text{coh}}(B = 0)}{\sqrt{1 + (ev_F c B \Gamma)^2}}. \quad (40)$$

where v_F is the Fermi velocity. If we increase B , the coherent part decreases, and, therefore, T_{\perp}^{max} would shift to *lower* values. A separation of the conductivity in two parts, as in Eq. (39), has been proposed previously² on a phenomenological basis, in order to describe the magnetoresistance of Sr_2RuO_4 (Except there a weak field de-

TABLE II: Temperatures scales obtained in the small polaron model applied to layered systems.

$\sigma_{coh} \sim \sigma_{incoh}$	GF coherence	Interlayer transport	Intralayer transport
T^*	$< k_B T^{coh} \sim \frac{\hbar\omega_0}{2g} \lesssim$	$k_B T_{\perp}^{max} \sim \frac{\hbar\omega_0}{\sqrt[4]{2^3}g}$	$< k_B T_{\parallel}^{max} \sim 2 \frac{\hbar\omega_0}{g}$

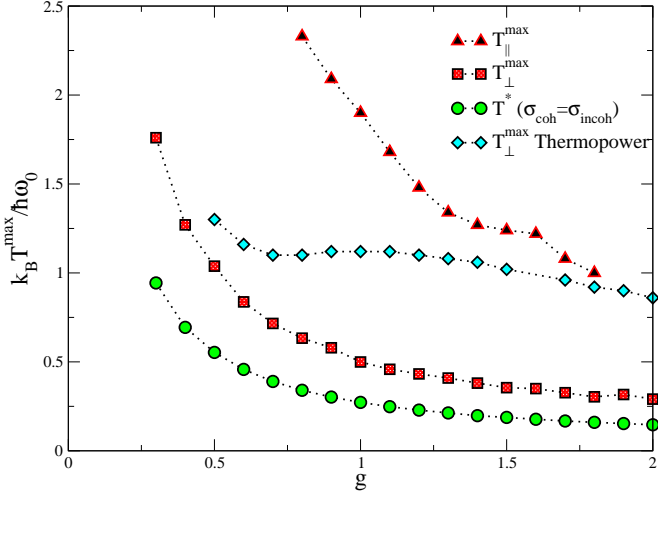
pendence is associated with the incoherent contribution due to Zeeman splitting).

V. DISCUSSION

We have presented a layered polaron model for systems consisting of two-dimensional layers coupled by tunneling. We have found that when the temperature is lower than the characteristic boson frequency the physics is dominated by coherent transport where the electrons scatters of bosons in the layers. Upon increasing the temperature a transition is made into a region where the physics is governed by incoherent small polarons. The small polarons are localized at the lattice sites and hop to new sites. We have extracted results for intralayer and interlayer transport, thermopower, ARPES, optical conductivity and magnetoresistance.

In Fig. 7 we plot the different crossover temperatures as a function of the dimensionless electron-boson coupling. The different temperature scales associated with small

FIG. 7: Crossover temperatures as a function of electron-phonon coupling constant, for the intralayer and interlayer resistivity, and the interlayer thermopower. For a fixed coupling and increasing temperature first the coherence between the layers is lost, then there is a crossover peak in the interlayer thermopower, and last the coherence within each layer is lost at elevated temperatures. The sequence of crossover does not change if t_{\parallel}/W is changed.



polaron transport is summarized in the table II.

The presented theory differs in the way polarons are formed from the theory by Ho and Schofield⁴². In their paper they assume that the polarons are formed from phonons traveling along the c -direction. Some of the results are similar, but in principle it is a different theory.

Acknowledgments

U. Lundin acknowledges the support from the Swedish foundation for international cooperation in research and higher education (STINT). This work was also supported by the Australian Research Council (ARC).

APPENDIX A: GREEN FUNCTION IN THE HIGH TEMPERATURE LIMIT

In order to calculate the intralayer conductivity at high temperatures, when polarons are formed and are localized, we need the GF. We perform perturbation theory in t and include the diagrams shown in Fig. 8. When



FIG. 8: The diagrams taken into account when calculating the self-energy for the trapped polaron in the high temperature limit.

summing the series shown in Fig. 8, we have to consider the lattice the electron moves in, i.e. the number of possible ways to return to the original site. In Fig. 9 we have shown the number of possible paths when the polaron hops 3 jumps away from its original site. We have to find a general expression for the number of possible jumps for the whole lattice, and take into account identical paths. Generally if the electron hops $2n$ steps, the number of

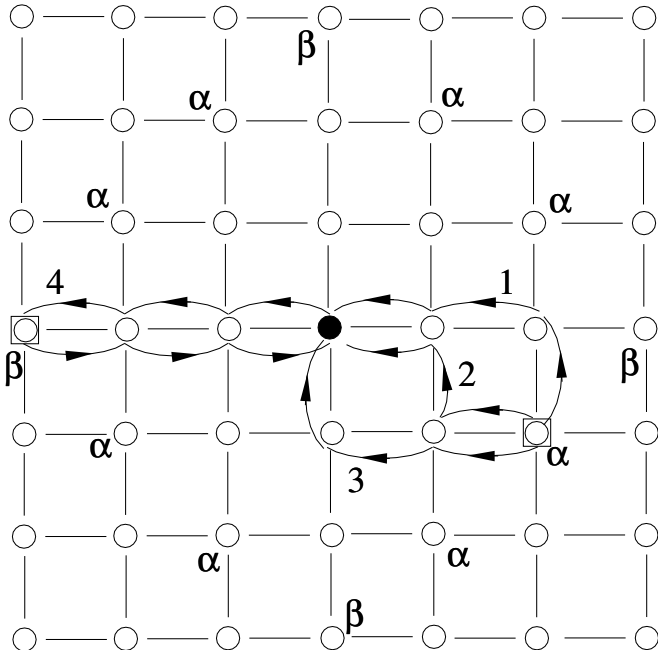


FIG. 9: Example when the polaron can hop 3 steps away, from the solid circle to the site marked with a box. From the sites marked with α there are 3 paths back (marked 1-3) and there are 3 paths there, there are 8 such equivalent α -sites. The polaron can also take the path to the site marked β , there are 4 equivalent sites of this type.

possible paths are $4+2\cdot 4n(n-1)$. Thus we get that the self energy is

$$\begin{aligned} \Sigma(\omega, \Gamma) &= 4 \sum_{n=1}^{\infty} [1 + 2n(1 - n)] t^{2n} G^{2n-1} \\ &= 4t^2 G \frac{1 + t^2 G^2 + t^4 G^4}{(1 - t^2 G^2)^3}, \end{aligned} \quad (A1)$$

where G is the local polaron GF, and t is the hopping integral within the layer.

* Electronic address: lundin@physics.uq.edu.au

¹ T. Kimura, Y. Tomioka, H. Kuwahara, A. Asamitsu, M. Tamura, and Y. Tokura, *Science* **274**, 1698 (1996).

² N. Hussey, A. Mackenzie, J. Cooper, Y. Maeno, S. Nishizaki, and T. Fujita, *Phys. Rev. B* **57**, 5505 (1998).

³ K. Takenaka, Y. Sawaki, and S. Sugai, *Phys. Rev. B* **60**, 13011 (1999).

⁴ T. Valla, P. Johnson, Z. Yusof, B. Wells, Q. Li, S. Loureiro, R. Cava, M. Mikami, Y. Mori, M. Yoshimura, et al., *Nature* **417**, 627 (2002).

⁵ M. Vozmediano, M. López-Sancho, and F. Guinea, *Phys. Rev. B* **68**, 195122 (2003).

⁶ A. Lavrov, M. Kameneva, and L. Kozeeva, *Phys. Rev. Lett.* **81**, 5636 (1998).

⁷ G. Mihály, I. Kézsmárki, F. Zámborszky, and L. Forró, *Phys. Rev. Lett.* **84**, 2670 (2000).

⁸ L. Buravov, N. Kushch, V. Merzhanov, M. Osharov, A. Khomenko, and E. Yagubskii, *J. Phys. I France* **2**, 1257

(1992).

⁹ J. Merino and R. McKenzie, Phys. Rev. B **61**, 7996 (2000).

¹⁰ A. Alexandrov and A. Bratkovsky, J. Phys.:Cond. Mat. **11**, 1989 (1999).

¹¹ M. Salamon and M. Jaime, Rev. Mod. Phys. **73**, 583 (2001).

¹² T. Palstra, A. Ramirez, S.-W. Cheong, B. Zegarski, P. Schiffer, and J. Zaanen, Phys. Rev. B **56**, 5104 (1997).

¹³ C.-J. Liu, C.-S. Sheu, and M.-S. Huang, Phys. Rev. B **61**, 14323 (2000).

¹⁴ X. Chen, C. Zhang, C. Almasan, J. Gardner, and J. Sarrao, Phys. Rev. B **67**, 94426 (2003).

¹⁵ S. Billinge, R. DiFrancesco, G. Kwei, J. Neumeier, and J. Thompson, Phys. Rev. Lett. **77**, 715 (1996).

¹⁶ C. Adams, J. Lynn, Y. Mukovskii, A. Arsenov, and D. Shulyatev, Phys. Rev. Lett. **85**, 3954 (2000).

¹⁷ B. Campbell, S. Sinha, R. Osborn, S. Rosenkranz, J. Mitchell, D. Argyriou, L. Vasiliu-Doloc, O. Seeck, and J. Lynn, Phys. Rev. B **67**, 020409 (2003).

¹⁸ E. Choi, J. Brooks, and J. Qualls, Phys. Rev. B **65**, 205119 (2002).

¹⁹ N. Mannella, A. Rosenhahn, C. Booth, S. Marchesini, B. Mun, S.-H. Yang, K. Ibrahim, Y. Tomioka, and C. Fadley, Phys. Rev. Lett. **92**, 166401 (2004).

²⁰ G. Mahan, *Many-Particle Physics* (Plenum Press, New York, 1990), 2nd ed.

²¹ J. Appel, *Solid State Physics*, Vol. 21 (Academic Press, New York and London, 1968).

²² S. Fratini and S. Ciuchi, Phys. Rev. Lett. **91**, 256403 (2003).

²³ X. Liu, H. Zhu, and Y. Zhang, Phys. Rev. B **65**, 024412 (2001).

²⁴ A. Alexandrov and A. Bratkovsky, Phys. Rev. Lett. **82**, 141 (1999).

²⁵ A. Alexandrov, G. Zhao, H. Keller, B. Lorenz, Y. Wang, and C. Chu, Phys. Rev. B. **64**, 140404 (2001).

²⁶ A. Weisse, J. Loos, and H. Fehske, Phys. Rev. B **68**, 024402 (2003).

²⁷ U. Lundin and R. McKenzie, Phys. Rev. B **68**, 081101 (2003).

²⁸ U. Lundin and R. McKenzie, cond-mat/0404528 (unpublished).

²⁹ T. Holstein, Ann. Phys. **8**, 343 (1959).

³⁰ I. Lang and Y. Firsov, Sov. Phys. JETP **16**, 1301 (1963).

³¹ A. Alexandrov and N. Mott, *Polarons and bipolarons* (World Scientific, Singapore, 1995).

³² E. B. Karlsson, *New perspectives on problems in classical and quantum physics* (Gordon and Breach, New York, 1998).

³³ S. Ciuchi, F. de Pasquale, S. Fratini, and D. Feinberg, Phys. Rev. B **56**, 4494 (1997).

³⁴ S. Wang, H. Yang, A. Sekharan, H. Ding, J. Engelbrecht, X. Dai, Z. Wang, A. Kaminski, T. Valla, T. Kidd, et al., Phys. Rev. Lett. **92**, 137002 (2004).

³⁵ P. Moses and R. McKenzie, Phys. Rev. B **60**, 7998 (1999).

³⁶ D. Adler, *Solid State Physics*, Vol. 21 (Academic Press, New York and London, 1968).

³⁷ D. Emin, Phys. Rev. Lett. **35**, 882 (1975).

³⁸ M. Jaime, M. Salamon, M. Rubinstein, R. Treece, J. Horowitz, and D. Chrisey, Phys. Rev. B **54**, 11914 (1996).

³⁹ T. Katsufuji, M. Kasai, and Y. Tokura, Phys. Rev. Lett. **76**, 126 (1996).

⁴⁰ K. Takenaka, Y. Sawaki, R. Shiozaki, and S. Sugai, Phys. Rev. B **62**, 13864 (2000).

⁴¹ A. J. Schofield and J. Cooper, Phys. Rev. B **62**, 10779 (2000).

⁴² A. Ho and A. Schofield, cond-mat/0211675 (unpublished).

⁴³ Strictly speaking there are three conditions for small polaron transport²⁹, $t < g\hbar\omega_0$, $\sqrt{2}t < M$, and $t < \sqrt{M} \left(\frac{2k_B T \hbar \omega_0}{\pi^3} \right)^{1/4}$.